Inorganic Chemistry
Article

Inorg. Chem. **2010**, *49*, 9321–9332 **9321**
DOI: 10.1021/ic100929f

Binding and Removal of Sulfate, Phosphate, Arsenate, Tetrachloromercurate, and Chromate in Aqueous Solution by Means of an Activated Carbon Functionalized with a Pyrimidine-Based Anion Receptor (HL). Crystal Structures of $[H_3L(HgCl_4)]\cdot H_2O$ and $[H_3L(HgBr_4)]\cdot H_2O$ Showing Anion$-\pi$ Interactions

Paloma Arranz,[†] Antonio Bianchi,[‡] Rafael Cuesta,[†] Claudia Giorgi,[‡] M. Luz Godino,[†] M. D. Gutiérrez,[†] Rafael López,*[,†] and Antonio Santiago[†]

[†]*Departament of Inorganic and Organic Chemistry, University of Jaén, 23071, Jaén, Spain, and*
[‡]*Department of Chemistry "Ugo Schiff", University of Florence, Via della Lastruccia 3, 50019 Sesto Fiorentino, Italy*

Received May 10, 2010

Binding of anions of great environmental concern such as SO_4^{2-}, PO_4^{3-}, AsO_4^{3-}, $HgCl_4^{2-}$, and CrO_4^{2-} by the protonated forms of a tren-like (tren = tris(2-aminoethyl)amine) ligand (HL) functionalized with a pyrimidine residue was studied by means of potentiometric measurements and isothermal titration calorimetry (ITC) affording log *K*, ΔH°, and $T\Delta S^\circ$ values for the formation of the relevant complexes. The complexes show high to very high stability due to the particular topology and electronic properties of the ligand which is able to use two separated coordination environments to host the anions, the protonated tren site where electrostatic and hydrogen bond interactions are operating, and the pyrimidine ring which may act via anion$-\pi$ interaction. A contribution of -8.9 ± 0.4 kJ/mol for pyrimidine$-$anion interaction in water was derived for SO_4^{2-} binding. The crystal structures of $[H_3L(HgCl_4)]\cdot H_2O$ (**1**), $[H_3L(HgBr_4)]\cdot H_2O$ (**2**), and that previously reported for $[H_3L(CdI_4)]$, clearly show these binding features in the solid state. A hybrid AC$-$HL material obtained by adsorption of HL on commercial activated carbon (AC) was used to study the removal of these anions from water. AC$-$HL shows enhanced adsorption capacity toward all the anions studied with respect to AC. This behavior is ascribed to the stronger interaction of anions with the HL function of AC$-$HL than with the Cπ-H_3O^+ sites of the unfunctionalized AC.

Introduction

Anion species are widely spread in both abiotic and biological systems and play important roles in many areas of industry, medicine, and agriculture.[1,2] For this reason, anion binding has attracted a great deal of interest. Although most research has focused on their binding to metal centers,[3−6] studies concerning the formation of supramolecular anion assemblies have grown steadily in the past few years.[7]

Formation of supramolecular anion species embodies an approach to obtain strong and selective anion binding based on noncovalent interactions with positively charged receptors. In this respect, it was proved that receptors based on polyammonium functions form very stable anion assemblies in aqueous medium via electrostatic and hydrogen bond interactions, although other noncovalent forces such as $\pi-\pi$ and anion$-\pi$ interactions, as well as solvophobic effects, can furnish significant contributions to their formation.[8−17]

*To whom correspondence should be addressed. E-mail: rlopez@ujaen.es.

(1) Sessler, J. L.; Gale, P. A.; Cho, W. S. *Anion Receptor Chemistry Monographs in Supramolecular Chemistry*; Stoddart, J. F., Ed.; RSC: Cambridge, UK, 2006.
(2) Bianchi, A.; Bowman-James, K. *Supramolecular Chemistry of Anions*; Garcia-España, E., Eds.; Wiley-VCH: New York, 1997.
(3) Schhmidtchen, F. P. *Coord. Chem. Rev*. **2006**, *250*, 2918.
(4) Amendola, V. I.; Fabbrizzi, L. *Chem. Commun*. **2009**, 513–531.
(5) O'Neil, E. J.; Smith, B. D. *Coord. Chem. Rev*. **2006**, *250*, 3068–3080.
(6) Rice, C. R. *Coord. Chem. Rev*. **2006**, *250*, 3190–3199.
(7) Special Issue on Anion Coordination Chemistry. *Coord. Chem. Rev*. **2006**, *250*, 2917−3244.
(8) Arranz, P.; Bencini, A.; Bianchi, B.; Díaz, P.; García-España, E.; Giorgi, C.; Luis, S. V.; Querol, M.; Valtancoli, B. *J. Chem. Soc., Perkin Trans*. **2001**, *2*, 1765–1770.
(9) Bazzicalupi, C.; Bencini, A.; Bianchi, A.; Cecchi, M.; Escuder, B.; Fusi, V.; Garcia-España, E.; Giorgi, C.; Luis, S. V.; Maccagni, G.; Marcelino, V.; Paoletti, P.; Valtancoli, B. *J. Am. Chem. Soc*. **1999**, *121*, 6807–6815.
(10) Clifford, T.; Danby, A.; Llinares, J. M.; Mason, S.; Alcock, N. W.; Powell, D.; Aguilar, J. A; García-España, E.; Bowman-James, K. *Inorg. Chem*. **2001**, *40*, 4710–4720.
(11) Bianchi, A; Micheloni, M.; Paoletti, P. *Inorg. Chim. Acta* **1988**, *151*, 269–272.
(12) Schneider, H. J.; Yatsimirsky, A. K. *Chem. Soc. Rev*. **2007**, *37*, 263–277.
(13) Garcia-España, E.; Díaz, P.; Llinares, J. M.; Bianchi, A. *Coord. Chem. Rev*. **2006**, *250*, 2952–2986.
(14) Kang, S. O.; Hossain, M. A.; Bowman-James, K. *Coord. Chem. Rev*. **2006**, *250*, 3038–3052.
(15) Bowman-James, K. *Acc. Chem. Res*. **2005**, *38*, 671–678. Kang, S. O.; Hossain, M. A.; Bowman-James, K. *Coord. Chem. Rev*. **2006**, *250*, 3038–3052.
(16) Llinares, J. M.; Powell, D.; Bowman-James, K. *Coord. Chem. Rev*. **2003**, *240*, 57–75.
(17) McKee, V.; Nelson, J.; Town, R. M. *Chem. Soc. Rev*. **2003**, *32*, 309–325.

© 2010 American Chemical Society
Published on Web 09/13/2010

Scheme 1

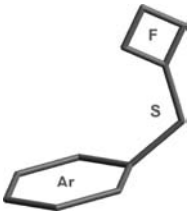

The design and synthesis of receptors capable of binding anionic guests are of considerable interest in the context of sensing and removal of environmental contaminants. Industrial, agricultural, and medicinal uses of anionic species determine their presence in soils, foods, and water, generating, in many cases, negative environmental effects.

In these cases, the use of anion binding materials represents a suitable approach for environmental decontamination. A strategy for decontamination of water is based on the attachment of anion binding groups to solid supports to obtain functionalized materials useful for waste anion removal.[18,19] In some earlier papers,[20−23] we reported on the syntheses of a series of molecular compounds based on highly electron-deficient pyrimidines (Ar) and containing different polyamine functions (F) linked to the C2′ pyrimidine atom through a nonaromatic spacer (S) (Scheme 1).

Adsorption of these compounds on a low-functionalized, commercially available activated carbon (AC) via irreversible π-stacking interaction between the pyrimidine residues and the arene centers of the graphite domains of AC provided new functionalized hybrid carbon materials whose surfaces are characterized by the chemical properties of the F function.[20,21,24,25] These functionalized materials showed enhanced ability in metal ions adsorption, with respect to the unmodified AC, due to the binding properties of the F functions.[21,22,25,26] In particular, the hybrid carbon material (AC−HL) containing the tren-like (tren = tris(2-aminoethyl)-amine) function HL (Scheme 2) proved to be efficient in the adsorption of both metal cations (Co^{2+}, Ni^{2+}, Cu^{2+}, Zn^{2+}, and Cd^{2+})[22,27] and CrO_4^{2-} anions,[20] because of the dual character of polyamine receptors which are able, depending

Scheme 2

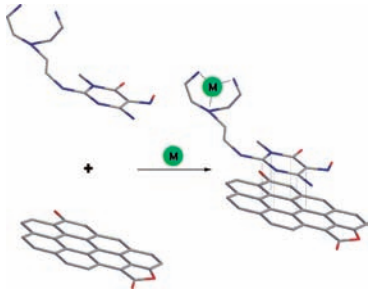

of their protonation state, to coordinate metal ions or to form supramolecular assemblies with anions.

This information, along with the knowledge that tren[28] and tren derivatives[29−36] are good anion receptors, prompted us to study the binding ability of HL, as well as of the hybrid material (AC−HL) obtained by adsorption of HL on a commercially available activated carbon, toward a series of inorganic anions of environmental interest (SO_4^{2-}, PO_4^{3-}, AsO_4^{3-}, $HgCl_4^{2-}$, and CrO_4^{2-}) with the aim of designing a suitable approach for the preparation of simple carbon based materials to remove anions from aqueous media.

We report here the results of this work.

Experimental Section

Materials. The ligand HL (6-amino-2-(2-(bis(2-aminoethyl)-amino)ethylamino)-3-methyl-5-nitrosopyrimidin-4(3H)-one)[37] and the AC−HL carbon-supported material[20] were prepared as previously described. High purity $Na_2HPO_4 \cdot 2H_2O$, Na_2SO_4, KH_2AsO_4, and $HgCl_2$ were purchased by Aldrich; KOH, NaOH, and K_2CrO_4 were purchased from Panreac; HCl, K_2SO_4, and KCl by Merck and KH_2PO_4 from Scharlau.

$[H_3L(HgCl_4)] \cdot H_2O$. Violet crystals of this compound suitable for X-ray analysis were obtained by slow evaporation of an aqueous solution containing H_3LCl_2, $HgCl_2$ (both 2.5×10^{-2} M), and NaCl (7.5×10^{-2} M) adjusted at pH 6.5 by the addition of 2 M KOH. $C_{11}H_{26}Cl_4N_8O_3Hg$: calcd. C 19.99, H 3.94, N 16.96; found C 19.77, H 3.76, N 16.75.

$[H_3L(HgBr_4)] \cdot H_2O$. Orange crystals of this compound suitable for X-ray analysis were obtained by slow evaporation of an aqueous solution containing H_3LCl_2, $HgCl_2$ (both 1.3×10^{-2} M), and KBr (0.5 M) after heating to 80 °C. $C_{11}H_{26}Br_4N_8O_3Hg$: calcd. C 15.75, H 3.10, N 13.36 ; found C 15.83, H 3.08, N 13.21.

(18) Sessler, J. L.; Samson, P. I.; Andrievsky, A.; Kral, V. *Supramolecular Chemistry of Anions. Application Aspects Involving the Supramolecualr Chemistry of Anions*. Wiley: New York, 1997; Chapter 10, pp 355−419.
(19) Special Issue. 35 Years of Synthetic Anion Receptor Chemistry. *Coord. Chem. Rev*. **2003**, *240* (1−2).
(20) García-Martín, J.; López-Garzón, R.; Godino-Salido, M. L.; Gutiérrez-Valero, M. D.; Arranz-Mascarós, P.; Cuesta, R.; Carrasco-Marín, F. *Langmuir* **2005**, *21*, 6908–6914.
(21) Gutiérrez-Valero, M. D; Godino-Salido, M. L.; Arranz-Mascarós, P.; López-Garzón, R.; Cuesta, R.; García-Martín, J. *Langmuir* **2007**, *23*, 5995–6003.
(22) García-Martín, J.; López-Garzón, R.; Godino-Salido, M. L; Cuesta, R.; Gutiérrez-Valero, M. D.; Arranz-Mascarós, P.; Stoeckli-Evans, H. *Eur. J. Inorg. Chem*. **2005**, 3093–3103.
(23) Gutiérrez-Valero, M. D., Personal Communication, University of Jaén, Jaén, 2009.
(24) García-Martín, J.; Godino-Salido, M. L.; López-Garzón, R.; Gutiérrez-Valero, M. D.; Arranz-Mascarós, P.; Stoeckli-Evans, H. *Eur. J. Inorg. Chem*. **2008**, 1095–1106.
(25) Gutiérrez-Valero, M. D.; Arranz-Mascarós, P.; Godino-Salido, M. L.; López-León, M. D.; López-Garzón, R.; Cuesta, R. *Microporous Mesoporous Mater*. **2008**, *116*, 445–451.
(26) Godino-Salido, M. L.; López-Garzón, R.; Arranz-Mascarós, P.; Gutiérrez-Valero, M. D.; Santiago-Medina, A.; García-Martín, J. *Polyhedron* **2009**, *28*, 3781–3787.
(27) García-Martín, J. *Doctorate Thesis*, University of Jaén, Jaén, 2006.
(28) Bazzicalupi, C.; Bencini, A.; Bianchi, A.; Danesi, A.; Giorgi, C.; Valtancoli, B. *Inorg. Chem*. **2009**, *48*, 2391–2398.
(29) Hossain, Md. A.; Liljegren, J. A.; Powell, D.; Bowman-James, K. *Inorg. Chem*. **2004**, *43*, 3751–3755.
(30) Bazzicalupi, C.; Bencini, A.; Berni, E.; Bianchi, A.; Ciattini, S.; Giorgi, C.; Maoggi, S.; Paoletti, P.; Valtancoli, B. *J. Org. Chem*. **2002**, *67*, 9107–9110.
(31) Beer, P. D.; Chen, Z.; Goulden, A. J.; Graydon, A.; Stokes, S. E.; Wear, T. *J. Chem. Soc., Chem. Commun*. **1993**, 1834–1836.
(32) Beer, P. D.; Hopkins, P. K.; McKinney, J. D. *Chem. Commun*. **1999**, 1253–1254.
(33) Valiyaveettil, S. K.; Engbersen, J. F. J.; Verboom, W.; Reinhoudt, D. N. *Angew. Chem., Int. Ed. Engl*. **1993**, *32*, 900–901.
(34) Kavallieratos, K.; Danby, A.; Van Berkel, G. J.; Kelly, M. A.; Sachleben, R. A.; Moyer, B. A. *Anal. Chem*. **2000**, *72*, 5258–5264.
(35) Raposo, C.; Álmaraz, M.; Martín, M.; Weinrich, V.; Mussóns, M. L.; Alcázar, V.; Caballero, M. C.; Morán, J. R. *Chem. Lett*. **1995**, 759–760.
(36) Ilioudis, C. A.; Tocher, D. A.; Steed, J. W. *J. Am. Chem. Soc*. **2004**, *126*, 12395–12402.
(37) Low, N. J.; López, M. D.; Arranz, P.; Cobo, J.; Godino, M. L.; López, R.; Gutiérrez, M. D.; Melguizo, M.; Ferguson, G.; Glidewell, C. *Acta Crystallogr. B* **2000**, *56*, 882–892.

Potentiometric Measurements. All pH-metric measurements ($pH = -\log[H^+]$) employed for the determination of equilibrium constants were carried out in 0.10 M KCl, 0.10 M KNO_3 (for CrO_4^{2-}), and 1.0 M KCl (for $HgCl_4^{2-}$) solutions at 298.1 ± 0.1 K, by using the equipment and the methodology that has been already described.[38] KNO_3 was employed in the case of CrO_4^{2-} to prevent the possible oxidation of the electrolyte, while 1.0 M KCl was used to ensure the complete formation of $HgCl_4^{2-}$. The system was calibrated as a hydrogen concentration probe by titrating known amounts of HCl with CO_2-free NaOH solutions and determining the equivalent point by Gran's method[39] which allows one to determine the standard potential E° and the ionic product of water ($pK_w = 13.83(1)$ (0.10 M KCl), 13.56(1) (0.10 M KNO_3), 13.79(1) (1.0 M KCl) at 298.1 ± 0.1 K). At least three measurements (about 100 data points each one) were performed for each system in the pH ranges 2.5−10.5. In all experiments, the ligand and anion concentration was about 1×10^{-3} M. The computer program Hyperquad[40] was used to calculate the equilibrium constants from emf data. Equilibrium constants involving anion protonation were redetermined under our experimental conditions (Table S1, Supporting Information).

Isothermal Titration Calorimetry (ITC). The enthalpies of ligand protonation and anion binding were determined in the same ionic media of potentiometric measurements by means of an automated system composed of a Thermometric AB thermal activity monitor (model 2277) equipped with a perfusion-titration device and a Hamilton Pump (model Microlab M) coupled with a 0.250 cm^3 gastight Hamilton syringe (model 1750 LT). The microcalorimeter was checked by determining the enthalpy of reaction of strong base (KOH) with strong acid (HCl) solutions. The value obtained (−56.7(2) kJ/mol) was in agreement with the literature values.[41] In a typical experiment, a KOH solution (0.10 M, addition volumes 15 μL) was added to acidic solutions of the ligand (5×10^{-3} M, 1.2 cm^3), containing equimolar quantities of the anion in the binding experiments. Corrections for heats of dilution were applied. The corresponding enthalpies of reaction were determined from the calorimetric data by means of the AAAL program.[42] In the case of chromate, precipitation occurring during the measurements prevented the determination of enthalpy changes.

ΔH° and $T\Delta S^\circ$ values for anions protonation were redetermined under our experimental conditions (Table S1, Supporting Information).

Spectrophotometric Measurements. Adsorption spectra of ligand/anion mixtures in a 1:1 molar ratio were recorded on a Perkin-Elmer Lambda-25 spectrophotometer. Spectra were obtained with 5×10^{-5} M (UV range) and 10^{-3} M (visible range) aqueous solutions (μ = 0.1 M KCl). HCl and KOH were used to adjust the pH, which was measured with a Crison 2002 micro-pH meter.

NMR Measurements. ^1H spectra of D_2O solutions were recorded at 298 K on a 400 MHz Bruker DPX300 spectrometer. In the pH-metric titrations, small amounts (2−10 μL) of NaOD or DCl solutions were added to adjust the pD. The pH was calculated from the measured pD values using the relationship pH = pD − 0.40.[43]

X-ray Crystallography. Suitable crystals of $[H_3L(HgCl_4)]\cdot H_2O$ (**1**) and $[H_3L(HgBr_4)]\cdot H_2O$ (**2**) were mounted on glass fibers and used for data collection. Crystallographic data for **1** and **2** were collected at room temperature with a Bruker Nonius Kappa CCD area diffractometer and a BRUKER SMART APEX diffractometer, respectively, by using Mo−Kα X-ray radiation (λ = 0.71073 Å). Multiscan absorption correction was carried out with SADABS 2.0.[44] Refinements were done with SHELXL-97[45] using a full-matrix least-squares on F^2. All hydrogen atoms were located in difference Fourier maps and included as fixed contributions riding on attached atoms with isotropic thermal displacement parameters of the respective atom. Final R_1(F), wR_2(F2), goodness-of-fit agreement factors, and details of the data collection and analyses for **1** and **2** can be found in Table 1. CCDC reference numbers are CCDC 768482 (**1**) and CCDC 768481 (**2**).

Table 1. Crystallographic Data and Structural Refinement Details for Compounds **1** and **2**

	1 $[H_3L(HgCl_4)]\cdot H_2O$	**2** $[H_3L(HgBr_4)]\cdot H_2O$
chemical formula	$C_{11}H_{26}Cl_4N_8O_3Hg$	$C_{11}H_{26}Br_4N_8O_3Hg$
M (g mol^{-1})	660.79	838.19
T (K)	293	293
λ (Å)	0.71073	0.71073
cryst syst	triclinic	triclinic
space group	$P\bar{1}$	$P\bar{1}$
a (Å)	8.058(5)	7.9806(8)
b (Å)	8.594(5)	8.9571(9)
c (Å)	16.215(5)	17.146(2)
α (deg)	81.915(5)	85.987(2)
β (deg)	81.079(5)	81.764(2)
γ (deg)	81.648(5)	82.079(2)
V (Å^3)	1089.5(10)	1199.8(2)
Z	2	2
F (g cm^{-3})	2.010	2.365
μ (mm^{-1})	7.583	13.107
no. of unique reflns	4965	5447
R(int)	0.0404	0.0371
$R_1{}^a$ [$I > 2\sigma(I)$]	0.0369	0.0346
$wR_2{}^a$ [$I > 2\sigma(I)$]	0.0714	0.0855

$^a R_1(F) = \Sigma||F_o| - |F_c||\Sigma|F_o|$; $wR_2(F^2) = [\Sigma w(F_o{}^2 - F_c{}^2)^2/\Sigma wF^4]^{1/2}$.

Preparation and Characterization of AC−HL. AC−HL was prepared by using a Merck K24504014 granulated activated carbon (AC) as starting material, whose composition, surface, and porosity properties had been determined in a previous work.[20] The required quantity of AC−HL was obtained by mixing AC with a 2.5 mM water solution of HL, keeping the relationship of 1 g of the former per 200 mL of the second. The mixture was left under stirring until the adsorption equilibrium was reached (3 days). Under these conditions (0.49 mmol HL/g AC), HL is irreversibly adsorbed (100%) on AC at any pH value.[20] The suspension was filtered and the solid residue was washed with distilled water and dried at 110 °C.

The specific surface area of AC−HL was determined as previously described[20] by applying the BET method[46] from the adsorption isotherm of N_2 on AC−HL obtained at 77 K. The total micropore volume of AC−HL was measured as the volume corresponding to the pores filled whit N_2 a 77 K, determined by applying the Dubinin−Radushkevich equation[47] to the same adsorption isotherm.

The surface charge of AC and AC−HL, at 291 K and different pH values, was determined by a procedure based on potentiometric titration data acquired by means of the apparatus

(38) Godino, M. L.; Gutiérrez, M. D.; López, R.; Moreno, J. M. *Inorg. Chim. Acta* **1994**, *221*, 177–181.
(39) Gran, G. *Analyst* **1952**, *77*, 661–671.
(40) Gans, P.; Sabatini, A.; Vacca, A. *Talanta* **1996**, *43*, 1739–1753.
(41) Hall, J. P.; Izatt, R. M.; Christensen, J. J. *J. Phys. Chem.* **1963**, *67*, 2605–2608.
(42) Vacca, A. *AAAL Program*, Department of Chemistry, University of Florence, Florence, 1997.
(43) Covington, A. K.; Paabo, M.; Robinson, R. A.; Bates, R. G. *Anal. Chem.* **1968**, *40*, 700–706.
(44) Sheldrick, G. M. *SADABS, Program for Empirical Adsorption Correction; Institute for Inorganic Chemistry*; University of Göttingen: Göttingen, Germany, 1996.
(45) Sheldrick, G. M. *SHELX 97, Program for Crystal Structure Refinement*; University of Göttingen: Göttingen, Germany, 1997.
(46) Adamson, A. W.; Gast. A. P. *Physical Chemistry of Surfaces*, 6th ed.; Wiley: New York, 1997.
(47) Bansal, R. C.; Goyal, M. *Activated Carbon Adsorption*; Taylor and Francis Group; CRC Press: New York, 2005.

above-described.[48,49] A suspension of the adsorbent (0.10 g) was prepared in 40 mL of 0.01 M NaCl solution and the pH was adjusted to about 3 by adding HCl. After 48 h of equilibration in a N_2 atmosphere, the suspension was titrated with 0.1 M NaOH up to pH 11. Equilibration times of 180 s were allowed to elapse between titrant additions (0.03 mL). In the case of AC−HL, it was verified by means of UV measurements that no release of HL occurred under these experimental conditions.

Titrations of a blank, consisting of 40 mL of 0.01 M NaCl solution to which the same amount of HCl was added as to the aforementioned suspension, were performed under the same conditions. From the proton balance provided by the titration data (presence of protonated and deprotonated sites) the surface charge density, Q, of the adsorbents was determined by using the equation:

$$Q = 1/m(V_o + V_t)([H]_i - [OH]_i - [H]_e + [OH]_e)$$

where V_o and V_t are the volumes of background electrolyte and added titrant, respectively, and m is the mass of the adsorbent. Subscripts i and e refer to concentrations of protons and hydroxyl groups in the blank (i) and in the suspension (e). Negative Q values (in proton equivalents per gram of adsorbent) indicate the predominance of deprotonated acidic sites whereas positive values indicate excess of protonated basic groups.

Adsorption Measurements. Anion solutions employed for the adsorption measurements were prepared by using K_2SO_4, K_2CrO_4, KH_2PO_4, and KH_2AsO_4 salts, while $HgCl_4^{2-}$ solutions were prepared by dissolving $HgCl_2$ in 1 M KCl. Equilibration times for adsorption measurements were preliminarily determined by means of independent experiments.[24] To this purpose, different flasks containing 50 mL of 10^{-3} M of anion (SO_4^{2-}, PO_4^{3-}, AsO_4^{3-}, CrO_4^{2-}, $HgCl_4^{2-}$) solution and 50 mg of adsorbent were prepared, kept under stirring, and the anion concentration was measured at different times by means of ICP-mass measurements. The anion adsorption isotherms were obtained at 298.1 ± 0.1 K. Typically, 50 mg of adsorbent (AC or AC−HL) was added to a 100 mL plastic flask containing 50 mL of aqueous solution containing the examined anion. Anion concentration was varied between 2×10^{-4} and 5×10^{-3} M, while the solution pH was selected, on the basis of the equilibrium data (see below), in order to have the uncharged complexes H_3L^{2+}-A^{2-} ($A^{2-} = SO_4^{2-}$, HPO_4^{2-}, $HAsO_4^{2-}$, CrO_4^{2-}) or the monocharged $[H_4L(HgCl_4)]^+$ (the only anion complex formed by $HgCl_4^{2-}$) as the predominant species in solution. The selected pHs were SO_4^{2-} (pH 6), HPO_4^{2-} (pH 7), $HAsO_4^{2-}$ (pH 7.5), CrO_4^{2-} (pH 7), $HgCl_4^{2-}$ (pH 5.5). The necessity to have these anions as predominant species in solution, avoiding the formation of dimeric or hydrolytic species, such as $Cr_2O_7^{2-}$ or HgOHCl and $Hg(OH)_2$, was also considered to select the pH for adsorption measurement with AC. The pH was initially adjusted by adding KOH or HCl to the adsorbate solutions. The anion concentration in the equilibrium solutions was determined by means of ICP-mass measurements.

UV measurements were performed to ascertain that no desorption of HL occurred in the presence of the studied anions under the experimental conditions employed, and blank experiments were performed to verify that neither the ligand nor the anions were adsorbed by the plastic flasks.

The XPS spectra obtained for the adsorption experiments of CrO_4^{2-} and $HgCl_4^{2-}$ on AC−HL were registered with a ESCA 5701 instrument (Physical Electronics), by using the Mgka 300w 15 kV radiation of twin anode in the constant analyzer energy mode, with pass energy of 187.85 eV (for the survey spectrum) and 29.35 eV (for narrow atomic ranges). Pressure of the analysis chamber was maintained at 4×10^{-9} Torr. The binding energy and the Auger kinetic energy scale were regulated by setting the C1s transition at 284.6 eV. The accuracy of BE values was ±0.2 eV.

Scheme 3

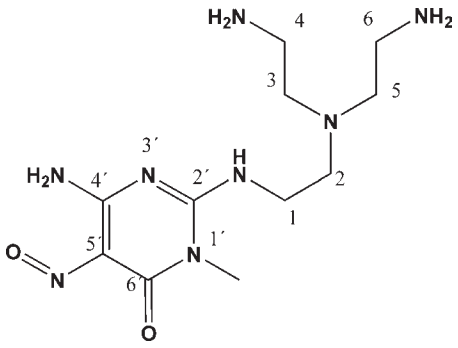

Calculation of Anion Radii. The Onsager radii of the anions[50] were determined in the gas phase at the PM3 semiempirical method.[51] The Gaussian03 program[52] was used to perform calculations. The adopted radii were calculated as those corresponding to the volume of the minimum energy conformer obtained after geometry optimization.

Results and Discussion

Protonation of HL. Protonation of HL (Scheme 3) in water, at 298 K (0.1 M KCl ionic strength) was reported previously.[20,22] L^- binds four protons in the 10.5 to 2.0 pH range.

Three of the protonation steps take place in the high pH range, which correspond to protonation of the $C(2')_{pyr}$-N^- amide anion (log K = 10.94) and the two primary amino groups (log K = 9.70 and 8.75), respectively. The fourth protonation step, which takes place by attachment of a proton to the σ electron pair on the nitrogen atom of the $C(5')_{pyr}O$ group (log K = 2.12),[22] was detected in the low pH range by UV spectroscopy. The $\Delta H°$ and $T\Delta S°$ parameters of ligand protonation (Table 2) were determined in this work. As can be seen from this table, all protonation reactions show high equilibrium constants and are exothermic as expected for protonation sites quite apart from each other.[53] A largely favorable entropic contribution was found for the first protonation step, in agreement with a large desolvation process accompanying the charge neutralization occurring upon protonation of the negatively charged (deprotonated) amide function. The decreasing entropy values for the successive protonation steps reflect an increasing ligand hydration due to the increase of ligand charge upon protonation.[53]

Crystal Structures of $[H_3L(HgCl_4)]\cdot H_2O$ and $[H_3L(HgBr_4)]\cdot H_2O$. The crystal structures of $[H_3L(HgCl_4)]\cdot H_2O$ (**1**) and $[H_3L(HgBr_4)]\cdot H_2O$ (**2**) complexes are shown in Figures 1 and 2. In both supramolecular complexes, the assembling of H_3L^{2+} and the tetrahalogenated anions is favored by a templating conformation of the flexible ligand, giving rise to second-sphere complexes. The protonated H_3L^{3+} ligand shows analogous conformations in both complexes and interacts with the anions through

(48) Bandosz, T.; Jagiello, J.; Contescu, C.; Schwarz, J. A. *Carbon* **1993**, *31*, 1193–1202.
(49) Jagiello, J.; Bandosz, T.; Schwarz, J. A. *Carbon* **1994**, *32*, 1026–1028.
(50) Onsager, L. *J. Am. Chem. Soc.* **1936**, *58*, 1482.
(51) Stewart, J. J. P. *J. Comput. Chem.* **1991**, *12*(3), 320–341.
(52) Frisch, M. J., Trucks, G. W. et al. Gaussian. Inc., Pittsburgh, PA, 2003.
(53) Bencini, A.; Bianchi, A.; García España, E.; Micheloni, M.; Ramirez, J. A. *Coord. Chem. Rev.* **1999**, *188*, 97–156.

Table 2. HL Protonation Constants, $\Delta H°$ and $T\Delta S°$ Values Determined in 0.10 M KCl Aqueous Solutions at 298.1 ± 0.1 K

	log K^a	$\Delta H°$ (kJ/mol)	$T\Delta S°$ (kJ/mol)
$L^- + H^+ = HL$	10.94(1)[b]	−9.30(1)	5.62(2)
$HL + H^+ = H_2L^+$	9.70(1)[b]	−13.5(1)	−0.3(1)
$H_2L^+ + H^+ = H_3L^{2+}$	8.75(1)[b]	−12.5(1)	−0.6(1)
$H_3L^{2+} + H^+ = H_4L^{3+}$	2.12(1)[b]	−5.50(1)	−2.61(2)

[a] Taken from ref 22. [b] Values in parentheses are standard deviations on the last significant figures.

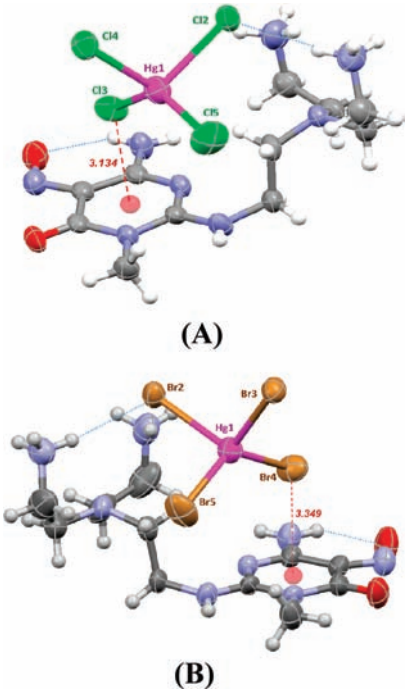

Figure 1. Perspective view of the asymmetric unit of (A) $[H_3L(HgCl_4)]\cdot H_2O$ (**1**) and (B) $[H_3L(HgBr_4)]\cdot H_2O$ (**2**).

hydrogen bonds between a protonated amine group and Cl2 (complex **1**) or Br2 (complex **2**) atoms, and further anion−π interactions occurring between the tetrahalogenated anions and the positive load of the ligand aromatic ring (Figure 1). The distances between the ring centroids and the anions, which are nested into the folded ligand, are 3.134 Å for chloride and 3.349 Å for bromide, and provide clear evidence for the existence of strong attractive anion−π interactions.[54]

Symmetry expansion of **1** and **2** results in 3D aggregations forming pairs of supramolecular complexes associated via $\pi-\pi$ interaction between the pyrimidine residues (Figure 2). For comparative purposes, this figure also includes the structure of the $[H_3L(CdI_4)]$ (**3**) complex, which was previously reported.[22] The $\pi-\pi$ interaction of adjacent ligands observed in the crystal structures of the three supramolecular complexes is similar to those described in the literature for pyrimidines.

With the aim of getting insight into the anion-pyrimidine interactions observed in the three crystal structures, we performed a comparative study between their geometrical features and those reported in the Cambridge Structural Database (CSD)[55] for analogous compounds.

(54) Ballester, P. *Struct. Bonding* (*Berlin*) **2008**, *129*, 127–174.
(55) Van de Streek, J. *Acta Crystallogr.* **2006**, *B62*, 567–579.

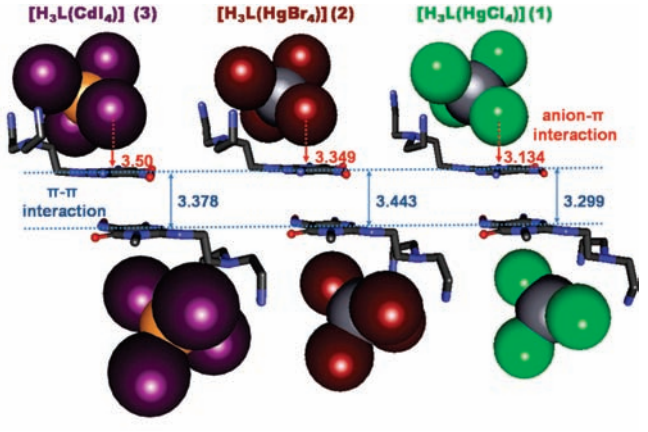

Figure 2. Schematic representation of the anion−π interactions (in red) and $\pi-\pi$ interactions (in blue) for complexes **1**, **2**, and **3**.

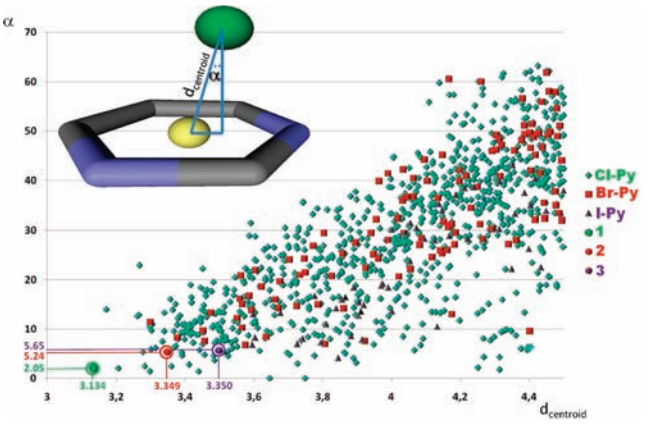

Figure 3. Representation of halide interactions (Cl, green; Br, red; I, violet) with pyrimidines from a CSD search.

Figure 3 shows a correlation between the distance of the anion from the pyrimidine centroid, $d_{centroid}$, and the α angle measuring the displacement of the anion from the perpendicular to the centroid. The figure collects data for all pyrimidine-halide (Cl, Br, I) interactions obtained from a CSD survey. An inspection to this figure allows us to compare both the strength and the geometry of the anion−π interactions. In most cases, anions tend to be positioned over the electron-deficient edge of the aromatic ring, as denoted by the large values of α and $d_{centroid}$. Conversely, in the case of **1**−**3**, the little α values show that the anions are positioned perpendicular to the pyrimidine plane over the centroid, which is consistent with anion−centroid distances shorter than those found for most of the analogous compounds in the CSD. In the case of compound **1**, the Cl−centroid distance (3.134 Å) is the shortest among all observed distances of this type.

In conclusion, the analysis of the crystallographic information obtained for **1**−**3** complexes shows a high sequestering capacity of H_3L^{2+} toward tetrahalogenated anions in the solid state.

Formation of Anion Complexes. The analysis of data obtained from the potentiometric titrations of HL/anion mixtures with 1:1 molar ratios, performed with the computer program Hyperquad[40] afforded the formation constants of the complexes in accordance to the equilibria $A^{n-} + L^- + mH^+ = (ALH_m)^{(m-n-1)+}$. Nevertheless, the formation constants obtained for these equilibria do not

Table 3. Stability Constants, $\Delta H°$ and $T\Delta S°$ Values of Anion Adducts and Hg(II) Complexes Determined in 0.10 M KCl Aqueous Solution at 298.1 K, unless Otherwise Noted

equilibria	log K	$\Delta H°$ (kJ/mol)	$T\Delta S°$ (kJ/mol)
$H_2L^+ + SO_4^{2-} = [H_2L(SO_4)]^-$	2.53(5)[a]	−5.0(4)	9.4(4)
$H_3L^{2+} + SO_4^{2-} = [H_3L(SO_4)]$	3.41(2)	−3.3(4)	16(1)
$H_4L^{3+} + SO_4^{2-} = [H_4L(SO_4)]^+$	4.42(2)	18.0(4)	43.2(4)
$H_3L^{2+} + HPO_4^{2-} = [H_3L(HPO_4)]$	3.02(1)	−2.5 (4)	15(1)
$H_3L^{2+} + H_2PO_4^- = [H_3L(H_2PO_4)]^+$	3.58(1)	−5.9(4)	14(1)
$H_4L^{3+} + H_2PO_4^- = [H_4L(H_2PO_4)]^{2+}$	4.86(1)	10.5(4)	38.2(4)
$H_3L^{2+} + HAsO_4^{2-} = [H_3L(HAsO_4)]$	2.89(1)	−9.6(4)	6.9(4)
$H_3L^{2+} + H_2AsO_4^- = [H_3L(H_2AsO_4)]^+$	3.11(3)	−23.0(4)	−5.2(4)
$H_4L^{3+} + H_2AsO_4^- = [H_4L(H_2AsO_4)]^{2+}$	4.55(2)	0.8(4)	27(1)
$L^- + Hg^{2+} = [HgL]^+$	6.99(7)[b]	−45.2(4)[b]	−5.3(4)[b]
$HL + Hg^{2+} = [HgLH]^{2+}$	6.14(6)[b]	−43.1(4)[b]	−8.1(4)[b]
$HgL^+ + OH^- = [HgL(OH)]$	3.07(1)[b]	5.0(4)[b]	22(1)[b]
$H_4L^{3+} + HgCl_4^{2-} = [H_4L(HgCl_4)]^+$	7.45(4)[b]	−1.7(4)[b]	41(1)[b]
$H_3L^{2+} + CrO_4^{2-} = [H_3L(CrO_4)]$	3.04 (2)[c]	*d*	*d*
$H_3L^{2+} + HCrO_4^- = [H_3L(HCrO_4)]^+$	3.98 (4)[c]	*d*	*d*
$H_4L^{3+} + HCrO_4^- = [H_4L(HCrO_4)]^{2+}$	5.41 (5)[c]	*d*	*d*
$H_4L^{3+} + Cr_2O_7^{2-} = [H_4L(Cr_2O_7)]^+$	8.42(5)[c]	*d*	*d*

[a] Values in parentheses are standard deviation on the last significant figures. [b] 1.0 M KCl. [c] 0.10 M KNO_3. [d] Not determined.

provide any information about the location of the m protons in the complex species. In the cases of the SO_4^{2-} and $HgCl_4^{2-}$ anions, which do not bear protonation in the studied pH range (2.5−10.5), the complexation equilibria can be described as the binding of the anion A^{2-} to the m-protonated ligand, for example, $A^{2-} + (H_mL)^{(m-1)+} = [A(H_mL)]^{(m-3)+}$. On the contrary, in the case of the CrO_4^{2-}, PO_4^{3-}, and AsO_4^{3-} anions, which suffers protonation in a wide pH range, additional experimental information is necessary to establish the distribution of protons in the different $(ALH_m)^{(m-n-1)+}$ complexes. ^1H and ^{13}C NMR measurements have proved very useful to this purpose.[8,9] In a previous study, the protonation pattern of HL in aqueous solution was established by using ^1H, ^{13}C NMR and UV−vis spectroscopic measurements.[22] Analogous measurements performed with the HL/anion mixtures (for PO_4^{3-}, AsO_4^{3-}, and CrO_4^{2-}) in 1:1 molar ratios (see Experimental Section), showed that the formation of $ALH_m^{(m-n-1)+}$ species do not modify the protonation behavior of the ligand, in any system, as shown in Figures S1 and S2, pointing out that the interacting species keep their basicity properties upon formation of the anion complexes. Hence, the location of the acidic protons in the complexes with SO_4^{2-}, PO_4^{3-}, AsO_4^{3-}, and CrO_4^{2-} was assumed to be regulated by the basicity of the interacting species and the relevant stability constants listed in Table 3 were calculated according to this role.

In the case of the $HL/HgCl_4^{2-}$ system, potentiometric measurements revealed that both anion complexes and metal complexes are formed (Figure 4). Indeed, ^1H NMR spectra showed an increasing shielding of protons of 3, 4, 5, and 6 methylene groups and an increasing deshielding of protons of 1 and 2 ones, related to the free ligand, as the pH increases above 7 (Figure 5). In the same pH domain, also the UV spectra of the $HL/HgCl_4^{2-}$ system, obtained in the 280−380 nm range at which the anion $HgCl_4^{2-}$ does not absorb, are quite different from those of the free ligand (Figure 6) in agreement with the formation of Hg(II) complexes by substitution of chloride anions in $HgCl_4^{2-}$ by nitrogen donor atoms of the ligand. Thus, both potentiometric and spectroscopic data demonstrate that at about pH 7 the ligand shifts its binding ability from

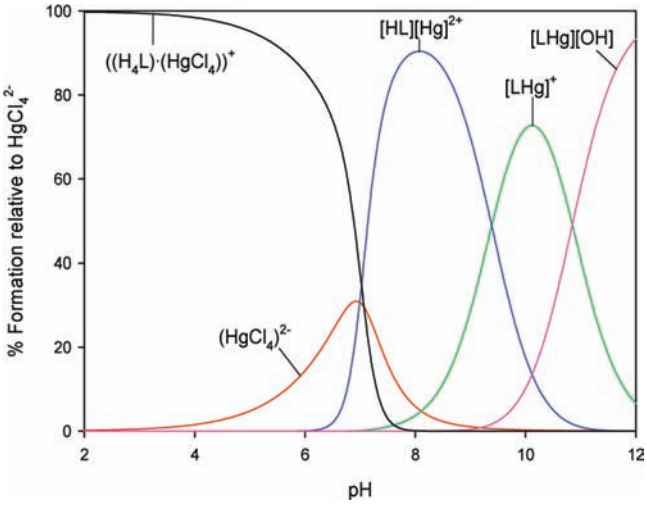

Figure 4. Species distribution plot for the $HL/HgCl_4^{2-}$ system in aqueous solution (1:1 molar ratio) as a function of pH, 1.0 M KCl at 298.1 ± 0.1 K.

the formation of second-sphere complexes with $HgCl_4^{2-}$ (pH < 7) to the formation of first-sphere ones with Hg(II) (pH > 7).

The stability constants of the complex species obtained by means of potentiometric measurements are listed in Table 3 and the species distribution plots for all the studied systems are showed in Figure S3, Supporting Information. As can be seen in this table, only anion complexes with 1:1 ligand-to-anion stoichiometry are formed. The stability of these complexes increases with increasing positive charge on the ligand and is promoted by predominant, favorable entropic contributions, as expected for association of species with opposite charges in a solvent of high dielectric constant like water.[2] The association gives rise to charge neutralization which is accompanied by a significant release of water molecules from the hydration spheres of the interacting species. Such desolvation process, which is endothermic (enthalpically unfavorable) but produces a considerable increase of translational entropy (entropically favorable), provides a significant contribution to the stability of anion complexes in water.

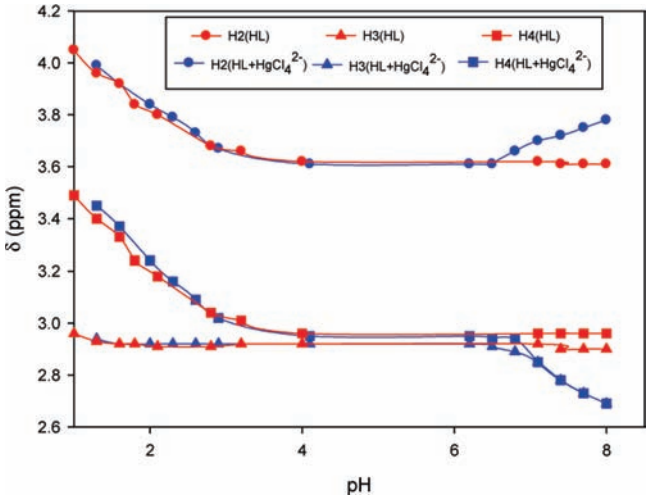

Figure 5. Chemical shifts of the ^{1}H NMR signals corresponding of the protons of 3, 4, 5, and 6 methylene groups of HL and HL−$HgCl_4^{2-}$ mixtures (1:1 molar ratio) vs pH.

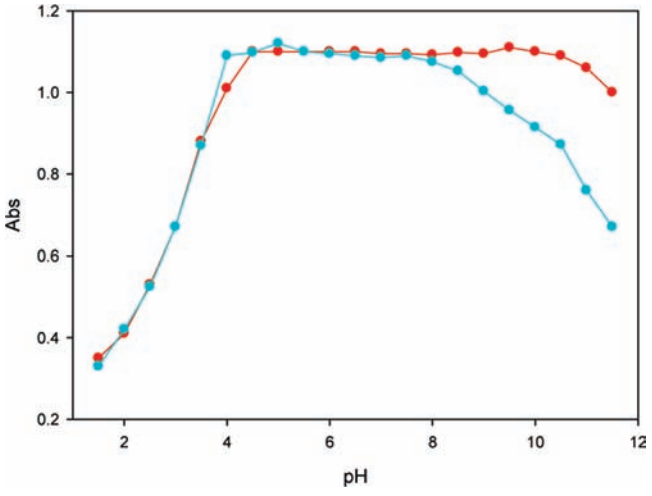

Figure 6. Absorbance values (λ = 330 nm) of HL (red) and HL-$HgCl_4^{2-}$ mixtures (1:1 molar ratio) (blue) in aqueous 1 M KCl solution vs pH.

In addition to electrostatic attraction, the formation of hydrogen bonds contribute to strengthen the association of anions with polyammonium receptors.[2,16] Seven types of hydrogen bonds can be formed in our anion complexes:

$$NH^+\cdots{}^-O \quad (1)$$

$$NH^+\cdots{}^-Cl \quad (2)$$

$$NH^+\cdots OH \quad (3)$$

$$N-H\cdots{}^-O- \quad (4)$$

$$N-H\cdots{}^-Cl \quad (5)$$

$$N-H\cdots OH- \quad (6)$$

$$N\cdots HO- \quad (7)$$

Types 1−6 involve the donor character of the ligand and the acceptor character of the anion, while in type 7 the ligand acts as an acceptor and the anion as a donor.

Since ammonium groups have enhanced hydrogen donor character related to the corresponding amino ones, the 1−3 hydrogen bond types are expected to be more effective than 4−6 ones. Hence, the increase of anion complex stability observed with increasing ligand charge (increasing protonation) is also promoted by the enhanced hydrogen donor properties of the ligand which are exerted through the formation of hydrogen bonds of 1−3 types. Since SO_4^{2-} and $HgCl_4^{2-}$ anions do not bear protonation over all of the studied pH range, hydrogen bonds of types 1 and 2 are the only hydrogen bonds contributions that can occur in their complexes. For the other anions, which suffer protonation, all types of hydrogen bonds are possible with the exclusion of 2 and 5. As shown before, hydrogen bonds of type 7 may be effective enough to modify the order of stability expected on the basis of plain electrostatic considerations.[9] Similar behavior is also found for some of the systems studied in this work. For instance, the $H_2PO_4^-$ anion interacts with H_3L^{2+} more strongly than the more charged HPO_4^{2-} (Table 3), in contrast with expectations based on electrostatic considerations. This behavior can be related to the greater ability of $H_2PO_4^-$ to act as hydrogen bond donor, which increases with anion protonation, acting though the formation of type 7 hydrogen bonds. This type of interaction takes place with partial proton transfer from $H_2PO_4^-$ to the ligand. Since all four protonation stages of the ligand are favorably exothermic (Table 2) and deprotonation of $H_2PO_4^-$ is almost athermic (Table S1, Supporting Information), type 7 hydrogen bonds in $[H_3L(H_2PO_4)]^+$ give rise to a favorable enthalpic contribution which enhances the complex stability (Table 3) with respect to $[H_3L(HPO_4)]$ (note that deprotonation of HPO_4^{2-} is endothermic (Table S1, Supporting Information)). Similar behaviors are shown by arsenate and chromate forms (Table 3).

It deserves to be highlighted that sulfate and phosphate complexes with the polyammonium forms of HL are significantly more stable than the analogous species formed by the parent ligand tren.[28] Similarly, the protonated species of HL bind sulfate more strongly than many other acyclic and even macrocyclic polyammonium receptors,[8] and form phosphate complexes which are in the higher range of stability observed for other acyclic polyammonium receptors.[9]

In previous works, it was evidenced that the aromatic residues of HL,[24] as well as those of previously studied HL analogues,[37,56,24] exhibit bipolar character with positive and negative charges located, respectively, at the ring and at the NO group attached to C(5′) of the pyrimidine ring. This suggests that in the anion complexes formed by H_2L^+ and H_3L^{2+}, the ligand might use two different coordination environments to host the anions, the polyammonium moiety, where electrostatic and hydrogen bond interactions are operating, and the pyrimidine ring which may act via anion−π interaction. Actually, in the crystal structures of H_3L^{2+} complexes with $HgCl_4^{2-}$, $HgBr_4^{2-}$ (described above), and that previously reported for CdI_4^{2-},[22] the receptor binds the

(56) Arranz-Mascarós, P.; Gutiérrez-Valero, M. D.; López-Garzón, R.; López-León, M. D.; Godino-Salido, M. L.; Santiago- Medina, A.; Stoekli-Evans, H. *Polyhedron* **2008**, *27*, 623–632.

anions through both such coordination environments, showing close contacts of the anions with the ring carbon atoms (anion-π interaction) and the polyammonium unit. Accordingly, HL appears to be a good receptor for these tetrahedral anions, thanks to its molecular topology and electronic properties, justifying the high stability of its anion complexes. Moreover, as protonation of N atom of C(5′)NO group occurring in H_4L^{3+} should enhance the amount and spreading of positive charge at the pyrimidine ring, it would be expected an additional positively charged site and stronger anion$-\pi$ interactions in H_4L^{3+} complexes with respect to H_3L^{2+}. This would explain the particularly high stability observed for $[H_4L(SO_4)]^+$, $[H_4L(H_2PO_4)]^{2+}$, $[H_4L(H_2AsO_4)]^{2+}$, $[H_4L(HgCl_4)]^+$, $[H_4L(HCrO_4)]^{2+}$, and $[H_4L(Cr_2O_7)]^+$ complexes (Table 3). Moreover, as protonation of the NO group takes place through the σ electron pair of the N atom,[57,58] it is to be expected an additional contribution of $NH^+\cdots{}^-X$ type to the stability of H_4L^{3+}complexes.

On the basis of the stability data determined for the formation of SO_4^{2-} complexes with the various protonated forms of HL, it is possible to demonstrate that the stability of these complexes is constituted by the contribution due to the formation of salt bridges and by an additional term that can be reasonably assigned to anion$-\pi$ interaction. On the same basis, it is possible to perform a rather confident evaluation of the energetic contribution for the anion$-\pi$ interaction occurring in these systems in solution. SO_4^{2-} is the only anion, among those studied here, which interacts with the receptor through the formation of salt bridges, with almost no possibility of proton transfer to the anion, and anion$-\pi$ interaction. The good linear correlation (R = 0.999, Figure S4, Supporting Information) exhibited by the binding free energies with the number of salt bridges formed in the complexes with H_2L^+, H_3L^{2+}, and H_4L^{3+}, corresponding to the receptor charge, according to the relationship $y = 5.4(\pm0.2)x + 8.9(\pm0.4)$ ($y = -\Delta G°$, x = number of salt bridges) furnishes two energetic contributions that can be referred to different binding forces. The first is the free energy increment for single salt bridge, of -5.4 ± 0.4 kJ/mol, which is in very good agreement with the value (-5 ± 1 kJ/mol) derived by Schneider[59] from a large number of equilibrium data, while the second is the residual free energy contribution at zero ligand charge ($x = 0$) of -8.9 ± 0.4 kJ/mol, not related to salt bridge formation, which can reasonably be ascribed to the anion$-\pi$ interaction. This value is one of the rare experimental evaluations of anion$-\pi$ association energy in solution. Very few free energy contributions for anion$-\pi$ interactions in solution were previously reported[59−61] to fall in the range from about −2.5 kJ/mol for a single anion−arene interaction in water/methanol (80/20)[59] to −9.9 kJ/mol for the interaction of Cl^- with a neutral tripodal aromatic receptor in benzene.[60] A similar value (about −8 kJ/mol) was obtained by means of ab initio calculations using benzene-chlorohydrocarbon model systems.[62]

For the $[H_4L(HgCl_4)]^+$ and $[H_4L(Cr_2O_7)]^+$ complexes, containing larger and poorly hydrated anions, higher stability was found in agreement with the lower energetic cost required for anion desolvation occurring upon interaction with the positively charged receptor. Finally, it is interesting to note that in the case of chromate, all species formed by this anion under different pH conditions, namely, CrO_4^{2-}, $HCrO_4^-$, and $Cr_2O_7^{2-}$, are bound by the different species formed by HL, which is a good prerequisite for the possible application of AC−HL sorbent for removal of these anions of great environmental concern from aqueous media in a large range of pH.

Table 4. Elemental Analysis of Activated Carbon

analysis (%)				
C	H	N	O[a]	ash
94.7	0.3	0.75	3.90	0.35

[a]Obtained by difference.

Characterization of the Adsorbents. The study of the adsorption of SO_4^{2-}, PO_4^{3-}, AsO_4^{3-}, CrO_4^{2-}, and $HgCl_4^{2-}$ required the previous characterization of the adsorbents AC and its functionalized AC−HL derivative. AC was characterized in a previous work.[20] It has a well developed specific surface area (1062 m^2/g), most of which (S_{mic} = 1000 m^2/g) corresponds to micropores, while a significant amount (S_{ext} = 62 m^2/g) corresponds to meso- and macropores.

As shown in Table 4, AC is mainly composed by C (94.7%) with negligible amounts of H (0.3%) and N (0.75%) and a small amount of O (3.90%). Studies performed by DTP and XPS techniques showed that the last minor component (O) is mainly found as carbonyl and quinone groups and, at lower extent, as carboxyl, lactone, and phenol groups.[20,21]

The plot of surface charge density, Q (in mmol of proton per g of sorbent), at the AC surface vs pH, calculated by means of the $Q = 1/m(V_o + V_t)([H]_i - [OH]_i - [H]_e + [OH]_e)$ equation (see Experimental Section), is shown in Figure 7. Positive Q values indicate that there is an excess of protonated sites compared to unprotonated ones, that is, there is a net positive charge at the AC surface. In contrast, a negative Q value indicates the prevalence of acidic sites.

The proton balance profile for AC (Figure 7) shows that the pH value at which Q becomes zero (the so-called point of zero charge), pH_{pzc} = 8.3, is considerably basic[20] accounting for the presence of a predominant amount of protonable basic sites at the sorbent surface. Thus, as none of the oxygen functional groups of AC exhibits noticeable proton affinity and the small amounts of lactone and phenolic functions have acidic character, the basic nature of the AC surface can be ascribed to the arene centers of the graphite sheets (C_π) which are protonated

(57) Low, J. N.; Quesada, A.; Glidewell, C.; Fontecha, M. A.; Arranz, P.; Godino, M. L.; López, R. *Acta Crystallogr.* **2002**, *E58*, o942–o945.
(58) López-Garzón, R.; Godino-Salido, M. L.; Arranz-Mascarós, P.; Fontecha-Cámara, M. A.; Gutiérrez-Valero, M. D.; Cuesta, R.; Moreno, J, M.; Stoeckli-Evans, H. *Inorg. Chim. Acta* **2004**, *357*, 2007–2014.
(59) Schneider, H.-J. *Angew. Chem., Int. Ed.* **1991**, *30*, 1417–1436.
(60) (a) Berryman, O. B.; Johnson, D. W. *Chem. Commun.* **2009**, 3143–3153. (b) Berryman, O. B.; Sather, A. C.; Hay, B. P.; Meisner, J. S.; Johnson, D. W. *J. Am. Chem. Soc.* **2008**, *130*, 10895–10897.
(61) Rosokha, Y. S.; Lindeman, S. V.; Rosokha, S. V.; Kochi, J. K. *Angew. Chem., Int. Ed.* **2004**, *43*, 4650–4652.
(62) Imai, Y. N.; Inoue, Y.; Nakanishi, I.; Kitaura, K. *Protein Sci.* **2008**, *17*, 1129–1137.

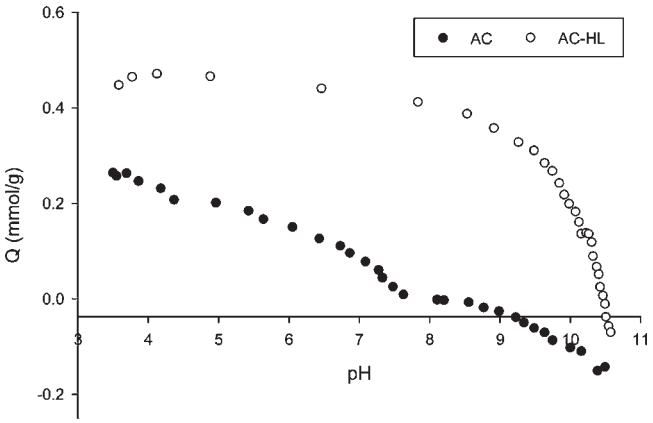

Figure 7. Proton balance profile for AC (solid circles) and for AC−HL (open circles).

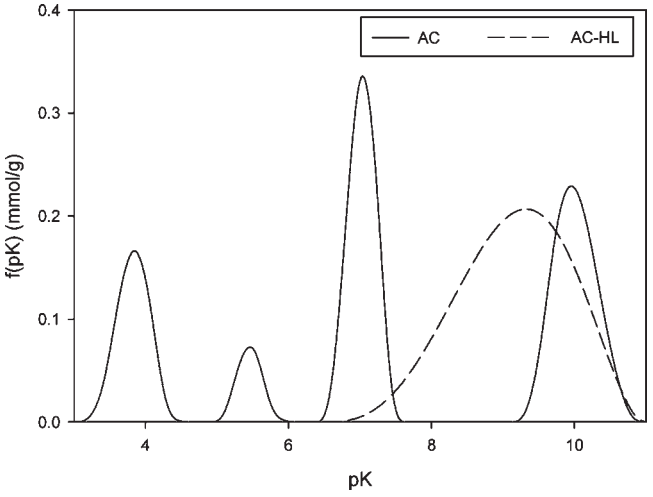

Figure 8. Distribution of acidity constants, $f(pK_a)$, for AC (solid lines) and for AC−HL (dashed lines).

according to the reaction:[63,64]

$$C_\pi + H_3O^+ \leftrightarrows C_\pi\text{-}H_3O^+$$

The numerical SAIEUS procedure was applied to the proton isotherm (Q vs pH) to determine the distribution of acidity constants, $f(pK_a)$, of the groups existing at the AC surface (Figure 8).[65,66] In accordance to this procedure, the pH values at which the peaks are centered provide information on the pK_a values of the acidic groups existing at the surface. Moreover, the area under the peaks corresponds to the total amount of each acidic function. According to literature data,[67] the peaks centered at pH values lower than 8 are consistent with the presence of carboxyl groups with different chemical environments at the AC surface. The amount of such functions (0.31 mmol/g), obtained by integrating the corresponding peaks, represents a little part of the total amount of oxygen existing in AC (2.43 mmol/g including

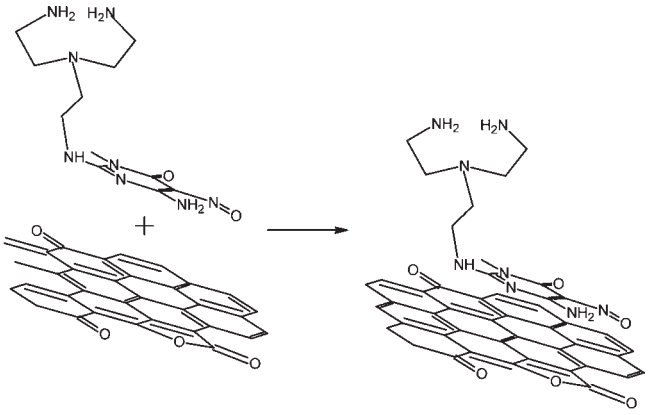

Figure 9. Development of triamine type functionalities on the activated carbon surface.

that of the water, 0.45 mmol/g, as determined by TG techniques). Deprotonation of these functions, which is complete at about pH 7.5, gives rise to negative charges at the AC surface. Hence, the existence of a net positive charge at the surface between pH 6 and 8.3 (Figure 7) points out the existence of further basic (neutral) sites, which are still protonated in this pH range, corresponding to the band centered at pK_a 7.02 in Figure 7 (0.18 mmol/g). As mentioned above, these sites are the arene centers, C_π, existing at the graphite sheets. Finally, the peak appearing at $pK_a = 9.97$ (0.18 mmol/g) can be assigned to phenol groups together with those coming from the hydrolysis of lactone functions.

Characterization of the AC−HL adsorbent showed that the main adsorption mechanism of HL on AC consists of a plane-to-plane $\pi-\pi$ interaction between the arene centers of AC and the pyrimidine aromatic moiety of HL.[20,21] The high irreversible character of this adsorption process is related to the strength of such $\pi-\pi$ interaction which is expected to have an important dispersion component[20,21] coupled with a strong polar interaction between the negative charge of the quadrupole moment of the arene centers[68] and the positive charge of the pyrimidine moiety of AC.[22] Combination of these binding interactions gives rise to a graphitized carbon material, which is quite stable to desorption in water, whose graphite sheets are functionalized with triamine receptor units (Figure 9).

The total surface area of AC ($S_{mic} + S_{ext} = 1062\ m^2/g$) diminishes considerably upon adsorption of HL on the graphite sheets (495 m^2/g) and also the pore volume suffers strong lowering (the micropore volume, corresponding to adsorption of N_2, decreases from 0.395 cm^3/g for AC to 0.187 cm^3/g for AC−HL) suggesting that also anion accessibility to the pores suffers some reduction.

The plot of Q vs pH for AC−HL is depicted in Figure 7. A comparison of this plot with the plot of Q vs pH for AC, shows widening of the pH domain in which Q is positive for AC−HL with respect to AC. Indeed, the pH_{pzc} value for the former, 10.4, is clearly higher than that for AC (8.3). Moreover, in the positive domain, Q values for AC−HL are clearly higher than for AC; that is, adsorption

(63) León y León, C. A.; Solar, J. M.; Calemna, V.; Radovic, L. R. *Carbon* **1992**, *30*, 797–810.
(64) Boehm, H. P. *Carbon* **1994**, 759–769.
(65) Jagiello, J. *Langmuir* **1994**, *10*, 2778–2785.
(66) Jagiello, J.; Bandosz, T.; Putyera, K.; Schwarz, J. *J. Colloid Interface Sci.* **1995**, *172*, 341–346.
(67) Dougherty, D. A. *Science* **1996**, *271*, 163–167.
(68) El-Sayed, Y.; Bandosz, T. *Phys. Chem. Chem. Phys.* **2003**, *5*, 4892−4898.

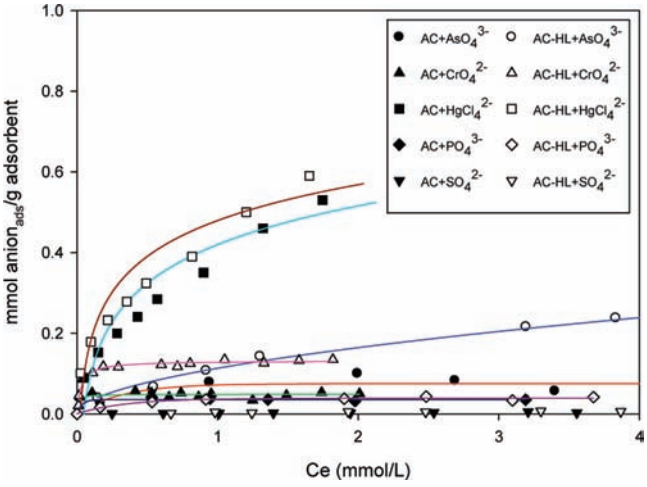

Figure 10. Adsorption isotherms of anions on AC (solid symbols) and on AC−HL (open symbols).

of HL on AC gives rise to a clear basicity enhancement. Application of the SAIEUS procedure to this last proton isotherm gives the distribution of acidity constants, $f(pK_a)$, reported in Figure 8.

This figure shows a unique broad band, spanning from pH 7.6 to 11.4 with a maximum at pH 9.9. All bands corresponding to protonation of arene centers and scarce carboxyl and lactone functions existing on AC surface have disappeared, in agreement with the involvement of arene centers in HL binding and with the reduced surface area of AC−HL with respect to the unfunctionalized AC. Deconvolution of this broad band (Figure S5, Supporting Information) showed that the main contributions to the basicity of AC−HL come from the primary amine functions and, at a largely lower extent, from the deprotonated amide groups of the adsorbed HL ligand, showing slightly lower basicity (protonation log K = 8.57, 9.54, and 10.63, respectively) with respect to their analogues in free HL (protonation log K = 8.75, 9.70, and 10.94, Table 2). Accordingly, the basicity enhancement observed for AC−LH can be ascribed to the prevailing effect of the triamine functionality and, in fact, the protonation path of AC−LH above pH 4 is quite similar to that of free HL.

Anion Adsorption by AC and AC−HL. Adsorption of SO_4^{2-}, PO_4^{3-}, AsO_4^{3-}, CrO_4^{2-}, and $HgCl_4^{2-}$ anions by AC and its functionalized AC−HL derivative was studied in aqueous solution at selected pH values (see Experimental Section). The corresponding adsorption isotherms are shown in Figure 10.

Adsorption mechanisms of inorganic anions on activated carbons depend on textural properties (surface area, pore size distribution) and chemical surface groups of the adsorbents.[69,70] In general, these mechanisms are based on noncovalent interactions, mainly electrostatic in nature, between anions and the positively charged basic sites existing on the adsorbent surface. Also dispersive force attraction with the arene centers of AC and hydrogen bonding with AC functional groups can contribute to anion retention.

Anion adsorption by the unfunctionalized AC was performed at pH values (see Experimental Section) corresponding to the presence on the AC surface of a net positive charge due to protonation of arene centers, which are expected to be the primary anion binding sites. As shown in Figure 10, the capacity of AC to adsorb the studied anions is low. For this reason, it was not possible to ascertain, by means of XPS spectra, if the oxidation state of CrO_4^{2-} was maintained after adsorption on AC. Conversely, in the case of $HgCl_4^{2-}$ adsorbed on AC, the existence of two bands in its XPS spectrum, at 100.7 eV (Hg4f 7/2) and 104.5 (Hg4f 5/2), demonstrates that all the mercury detected by this technique was Hg(II). Moreover, the value found in this spectrum for [Cl]/[Hg] molar ratio was close to 4, suggesting that the mercury detected was actually as $HgCl_4^{2-}$ anion.

As XPS characterizes the surface to a depth of a few nanometers, these results point out that $HgCl_4^{2-}$ is actually the adsorbed species existing in the outer surface of AC; that is, reduction of Hg(II) occurs on it. Nevertheless, the possibility that reduction of metal ions may have occurred within the deeper narrow pores cannot be excluded.

Fitting of the AsO_4^{3-}, CrO_4^{2-}, and $HgCl_4^{2-}$ adsorption isotherms (Figure 9), performed by using the Langmuir equation, afforded the values of maximum adsorption capacity (X_m) of AC which define the sequence ${}^{AC}X_{m_{SO_4^{2-}}}$, ${}^{AC}X_{m_{HPO_4^{2-}}} \ll {}^{AC}X_{m_{CrO_4^{2-}}}$ (0.07 mmol/g) $\approx$ ${}^{AC}X_{m_{HAsO_4^{2-}}}$ (0.08 mmol/g) $<$ ${}^{AC}Xm_{HgCl_4^{2-}}$ (0.55 mmol/g). This sequence, showing marked selectivity in the adsorption of the anions of greater environmental concern, seems to be regulated by the hydrophobic character of anions, as predicted by the Hofmeister series,[71] according to the rather general role that anions which interact less with water are better extracted from water. However, the hydrophobic character, or the hydration energy of $HgCl_4^{2-}$, as well as its collocation in the Hofmeister series are not known. An estimation of the hydration energy of these anions can be made by means of the Latimer equation (ΔH_{hyd} = 57.000 Z^2/r, in kJ/mol),[72] provided that the anion radii are known, which predicts that for anions of equal charge the hydration energy decreases with increasing anion radius. The Onsager anion radii, calculated as reported in the Experimental Section, are $r_{CrO_4^{2-}}$ = 3.878 Å $<$ $r_{HAsO_4^{2-}}$ = 3.957 Å $<$ $r_{HgCl_4^{2-}}$ = 4.604 Å, then the hydration energies of these anions are expected to decrease in the opposite order. Consequently, $HgCl_4^{2-}$ appears to be significantly more hydrophobic (less hydrated) than the other anions, in particular with respect to sulfate and phosphate which are known to have very high hydration energy,[73] confirming that the observed adsorption capacity of AC is strictly correlated with the hydrophobic nature of the considered anions. However, also the larger positive charge density existing at the AC surface at the pH adopted for $HgCl_4^{2-}$ adsorption (pH 5, Figure 6) furnishes an important contribution to the widely higher adsorptivity of AC toward $HgCl_4^{2-}$.

(69) Radovic, L.; Moreno-Castilla, C.; Rivera-Utrilla, J. *Chemistry and Physics of Carbon*; Radivic, L., Eds.; Marcel Dekker: New York, 2000; Vol. *27*.
(70) Radovic, L. R.; Silva, I. F.; Ume, J. I.; Menéndez, J. A.; Leon y Leon, C. A.; Scaroni, A. W. *Carbon* **1997**, *35*, 1339–1348.
(71) Hofmeister, F. *Arch. E. Pathol. Pharmakol.* **1888**, *24*, 247–260.
(72) Wulfsberg, G. *Inorganic Chemistry*; University Science Book: Herndon, VA, 2000; Chapter 2.
(73) Marcus, Y. *Ion Solvation*; Wiley: New York, 1985.

Also the isotherms of anion adsorption on AC−HL are depicted in Figure 10. As can be seen in this figure, in spite of the pore blocking produced by adsorption of HL over AC, the adsorption capacities of HL−AC toward the studied anions increases compared to AC. The increase, however, is large only for $HAsO_4^{2-}$ and CrO_4^{2-} while it is small for $HgCl_4^{2-}$ and very small for HPO_4^{2-} and SO_4^{2-}. By using XPS spectra, it was possible to obtain information on the oxidation state of the chromium adsorbed on AC−HL. In the case of a sample of CrO_4^{2-}, adsorbed from water at pH 7.0, a band (weak) at 578.5 eV, which can be assigned to the Cr_{2p} of Cr(VI), and the absence of bands in the 575.5−577.6 eV range of binding energies indicated that reduced chromium (0) is not present;[74] that is, it was adsorbed as CrO_4^{2-}. Analogously, the existence of two bands at 100.7 eV (Hg4f 7/2) and 104.7 eV (Hg4f 5/2) in the XPS spectra of the AC−HL/$HgCl_4^{2-}$ material, assignable to Hg(II), proved that none of the anion detected by this technique was reduced upon adsorption. Moreover, the value of the [Cl]/[Hg] molar ratio obtained from the mentioned spectra was 3.7. Thus, similarly to the case of AC, these results point out that CrO_4^{2-} and $HgCl_4^{2-}$ are actually the adsorbed species existing at the outer surface of AC−HL; that is, reduction of these oxidized metal ions does not occur. Nevertheless, the possibility that such reduction may have occurred within the deeper unfunctionalized narrow pores cannot be excluded. However, it seems likely that, in the case of this adsorbent, blocking of the entrance to the narrow pores by the adsorbed HL molecules (which is suggested by the reduction of the surface area of AC upon adsorption of HL) minimizes the possibility of metal reduction into the pores.

The enhancement of anion adsorption capability shown by AC−HL with respect to AC is consistent with the higher density of positive charge on the AC−HL surface, in the 5.0−7.5 pH range (Figure 7). Thus, it can be expected that such enhancement increases with the differences between surface charge densities of AC−HL and AC. The adsorption isotherms reported in Figure 10 are reasonably well fitted by the Langmuir equation (R^2 varied between 0.9626 and 0.9931) affording the relevant maximum adsorption capacities. The values obtained (in mmol of anion per gram of AC−HL) are $^{AC-HL}Xm_{SO_4^{2-}}$ = 0.0093 mmol/g, $^{AC-HL}Xm_{HPO_4^{2-}}$ = 0.0436 mmol/g, $^{AC-HL}Xm_{CrO_4^{2-}}$ = 0.125 mmol/g, $^{AC-HL}Xm_{HAsO_4^{2-}}$ = 0.211 mmol/g, and $^{AC-HL}Xm_{HgCl_4^{2-}}$ = 0.674 mmol/g, as expected on the basis of anion hydrophobicity growing in the same order.

The increase of the maximum adsorption capacities of AC−HL, relative to AC, toward $HAsO_4^{2-}$, CrO_4^{2-}, and $HgCl_4^{2-}$, expressed as $^{AC-HL}Xm/^{AC}Xm$, follows the sequence 2.68 ($HAsO_4^{2-}$) > 1.69 (CrO_4^{2-}) > 1.23 ($HgCl_4^{2-}$). As expected, this order is the same shown by the difference in surface density of positive charge (ΔQ) between AC−HL and AC, calculated from data in Figure 7 at the pH values of the adsorption experiments: $\Delta Q_{HAsO_4^{2-}}$ (pH 7.5) = 0.40 mmol/g > $\Delta Q_{CrO_4^{2-}}$ (pH 7.0) = 0.36 mmol/g > $\Delta Q_{HgCl_4^{2-}}$ (pH 5.1) = 0.26 mmol/g. Since the positively charged sites on AC−HL surface at these pH values are the completely protonated triamine functions, the enhanced adsorption capacities of AC−HL toward the studied anions can be related to the stronger interaction of anions with the protonated triamine functions with respect to the protonated Cπ-H_3O^+ sites of AC, the relatively small increment of the maximum adsorption capacity toward $HgCl_4^{2-}$ of AC−HL, related to AC, being explained by the little value of ΔQ at pH 5.1.

As stated above (see Experimental Section), the values of the working pH for the adsorption experiments were selected in order to have the uncharged complexes H_3L^{2+}-A^{2-} (A^{2-} = SO_4^{2-}, HPO_4^{2-}, $HAsO_4^{2-}$, CrO_4^{2-}) or the monocharged $[H_4L(HgCl_4)]^+$ (the only anion complex formed by $HgCl_4^{2-}$) as the most abundant species in solution. Assuming that the predominant adsorption mechanism of anions on AC−HL is the interaction with the protonated triamine function, the maximum adsorption capacity toward a given anion (A^{2-}) is expected to be determined by the balance of two opposite contributions: the favorable interaction between H_3L^{2+} and A^{2-}, and the unfavorable desolvation process occurring upon formation of the H_3L^{2+}-A^{2-} complex. The desolvation effect can be regarded as composed of two parts: one is determined by the release of solvent molecules occurring when the anion interacts with the free receptor, and the other one is caused by the release of further solvent molecules taking place at the hydrophobic surface of AC. The effect of the first desolvation part is included in the values of the association constants of the different anion complexes, which appear not to be much differentiated by this contribution since the association constants of the H_3L^{2+}-A^{2-} species are quite similar. Only the association constant for the $[H_4L(HgCl_4)]^+$ species (log K = 6.93) seems to be favored by the poor solvation of the large $HgCl_4^{2-}$ anion, although the greater charge on the receptor (H_4L^{3+}) must furnish a primary contribution to the high association constant. Hence, under the assumption that the interaction of HL with AC does not change much the binding ability of HL and the eventual changes are equal for the different anions, the maximum adsorption capacity (Xm) of AC−HL seems to be strongly affected by the desolvation process occurring when the anions are attracted in proximity of the hydrophobic AC surface. The accessibility to this hydrophobic region is expected to be easier for the less solvated anions and, accordingly, the X_m values increase with increasing hydrophobic character of these anions. Hence, the considerably higher X_m value obtained for $HgCl_4^{2-}$ can be ascribed to the high association energy of the $[H_4L(HgCl_4)]^+$ species which is poorly opposed by the low energetic cost necessary to desolvate the large and weakly solvated $HgCl_4^{2-}$ anion.

Concluding Remarks

Protonated forms of the ligand HL have two separated environments that can be used to host anions, the polyammonium moiety, where electrostatic and hydrogen bond interactions are operating, and the pyrimidine ring which acts via anion−π interaction. Protonation of the pyrimidine C(5′)NO group, taking place in the fourth protonation stage, enhances the positive charge on the pyrimidine ring increasing the ligand ability to form anion−π interactions. A contribution of −8.4 ± 0.4 kJ/mol for pyrimidine−anion interaction in water was derived for SO_4^{2-} binding. Accordingly,

(74) http://www.lasurface.com/database/spectrexps.php.

HL appears to be a good receptor for these tetrahedral anions (SO_4^{2-}, PO_4^{3-}, AsO_4^{3-}, $HgCl_4^{2-}$, CrO_4^{2-}), thanks to its molecular topology and electronic properties, its protonated species being able to form stable to very stable complexes with the studied anions. These are good prerequisites to achieve efficient anion binding and removal from aqueous media with the functionalized AC−HL sorbent. Indeed, AC−HL shows increased adsorption capacity toward dinegative forms all these anions (SO_4^{2-}, HPO_4^{2-}, $HAsO_4^{2-}$, $HgCl_4^{2-}$, CrO_4^{2-}), compared with AC. The irreversible adsorption of HL on AC gives rise to a marked enhancement of the positive charge density of the hybrid material (AC−HL) with respect to AC, in the 3−10 pH range, due to the presence of the protonated forms of the HL functionality, which offer a better anchorage to anions than the Cπ-H_3O^+ sites of AC. Nevertheless, a crucial contribution to the adsorption capacity is given by the hydrophobic character of the anions, which increases with increasing anion radius. Accordingly, largely greater maximum adsorption is observed for the larger, poorly solvated, $HAsO_4^{2-}$, $HgCl_4^{2-}$, and CrO_4^{2-} anions. Furthermore, X-ray structures of the $HgCl_4^{2-}$ and $HgBr_4^{2-}$ complexes show the existence of anion−π accompanied by hydrogen-bonding interactions as a robust structural motif of the solid-state packing. This is an example of a system in which a simple and flexible ligand adapts its conformation to respond to the demands of the coordinated anions.

To the best of our knowledge, the present results, together with other ones previously obtained,[20−26] establish for the first time a rational method to achieve functionalization of suitable activated carbons, by adsorption of molecular receptors like HL, to achieve anion adsorption from water.

These results stimulate further studies to get more insight into the factors determining the adsorbent capacity of similar hybrid material toward anions, in particular, concerning the topological and electronic properties of the functionalities in addition to the textural characteristics of the carbon support.

Supporting Information Available: Crystallographic files in CIF format. Tables listing detailed crystallographic data, atomic positional parameters, anisotropic temperature factors, and bond distances and angles for $[H_3L(HgCl_4)]$ and $[H_3L(HgBr_4)]$ complexes. Thermodynamic parameters for anion protonation. Chemical shifts vs pH for ^{1}H-RMN signals of HL and HL/anion mixtures in the cases of SO_4^{2-}, PO_4^{3-}, AsO_4^{3-}, and CrO_4^{2-} anions. Chemical shifts vs pH of the visible maximum from pH 1.5 to pH 6 for all systems. Species distribution plot for all complex systems in aqueous solution. Linear correlation between free energies change for SO_4^{2-} complexation and ligand charge. Deconvolution of the distribution of acidity constants, $f(pK_a)$, for AC−HL. CCDC reference numbers for crystallographic files are CCDC 768482 (**1**) and CCDC 768481 (**2**). This material is available free of charge via the Internet at http://pubs.acs.org.